Mapping the Visual Field to the Optic Disc in Normal Tension Glaucoma Eyes

David F. Garway-Heath, FRCOphth,[1] Darmalingum Poinoosawmy, BSc,[1] Frederick W. Fitzke, PhD,[2] Roger A. Hitchings, FRCOphth[1]

Purpose: To establish the anatomical relationship between visual field test points in the Humphrey 24-2 test pattern and regions of the optic nerve head (ONH)

Design: Cross-sectional study.

Participants: Glaucoma patients and suspects from the Normal Tension Glaucoma Clinic at Moorfields Eye Hospital.

Methods: Sixty-nine retinal nerve fiber layer (RNFL) photographs with well-defined RNFL defects and/or prominent bundles were digitized. An appropriately scaled Humphrey 24-2 visual field grid and an ONH reference circle, divided into 30° sectors, were generated digitally. These were superimposed onto the RNFL images. The relationship of visual field test points to the circumference of the ONH was estimated by noting the proximity of test points to RNFL defects and/or prominent bundles. The position of the ONH in relation to the fovea was also noted.

Main Outcome Measures: The sector at the ONH corresponding to each visual field test point, the position of the ONH in relation to the fovea, and the effect of the latter on the former.

Results: A median 22 (range, 4–58), of a possible 69, ONH positions were assigned to each visual field test point. The standard deviation of estimations was 7.2°. The position of the ONH was 15.5° (standard deviation 0.9°) nasal and 1.9° (standard deviation 1.0°) above the fovea. The location of the ONH had a significant effect on the corresponding position at the ONH for 28 of 52 visual field test points.

Conclusions: A clinically useful map that relates visual field test points to regions of the ONH has been produced. The map will aid clinical evaluation of glaucoma patients and suspects, as well as form the basis for investigations of the relationship between retinal light sensitivity and ONH structure. *Ophthalmology 2000;107: 1809–1815 © 2000 by the American Academy of Ophthalmology.*

Primary open-angle glaucoma is the term given to a progressive optic neuropathy in which a functional deficit, measurable as visual field loss, is associated with morphologic changes that occur at the optic nerve head (ONH) and retinal nerve fiber layer (RNFL).

The relationship between localized visual field defects and discrete RNFL loss has been investigated by means of high-resolution perimetry, and the topography of the RNFL defect and the functional abnormality have been shown to be closely related.[1–3] However, the correspondence between ONH changes and functional deficits is less well established.

Structural damage in glaucoma is frequently quantified by measurements of the area of the neuroretinal rim from magnification-corrected measurements of fundus photographs (planimetry)[4–6] and images from scanning laser ophthalmoscopes.[7,8] It has been demonstrated in experimental primate glaucoma that the area of the neuroretinal rim, measured in vivo from stereoscopic photographs and scanning laser tomographic images, is related to axon numbers measured histologically.[9,10]

It is desirable to establish the topographic correspondence between ONH and visual field regions. This correspondence may shed light on the relationship between structural and functional changes in primary open-angle glaucoma, and possible differences in the relationship between the two in different parts of the visual field or ONH. In addition, concordance between structural and functional findings will be of use in clinical practice.

The precise relationship between visual field locations and corresponding regions of the ONH is poorly documented. Wirtschafter et al[11] published a "profile of nerve fiber function in optic disc sectors," in which regions of the visual field were related to optic disc sectors. The boundaries of the visual field regions were derived from illustrations of the primate nerve fiber layer. Weber et al,[12] Yam-

Originally received: September 3, 1999.
Accepted: May 3, 2000. Manuscript no. 99603.

[1] Glaucoma Unit, Moorfields Eye Hospital, London, England.

[2] Department of Visual Science, Institute of Ophthalmology, London, England.

Presented in part at the Glaucoma Society (UK & Eire) Annual Meeting, London, England, November 1998.

D. F. Garway-Heath is funded by the BUPA Fellowship (Royal College of Ophthalmologists/BUPA) and the David Cole Travel Award (Glaucoma Society (UK & Eire)/Merck Sharp & Dohme).

The authors have no proprietary interest in the development or marketing of any product or instrument mentioned in this article.

Reprint requests to D. F. Garway-Heath, Glaucoma Unit, Moorfields Eye Hospital, City Road, London, EC1V 2PD, England.

ISSN 0161-6420/00/$–see front matter
PII S0161-6420(00)00284-0

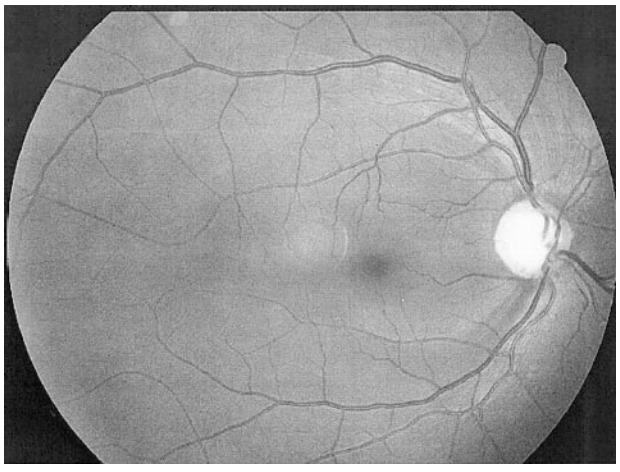

Figure 1. Example of a retinal nerve fiber layer photograph of an eye with well-defined nerve fiber layer defects.

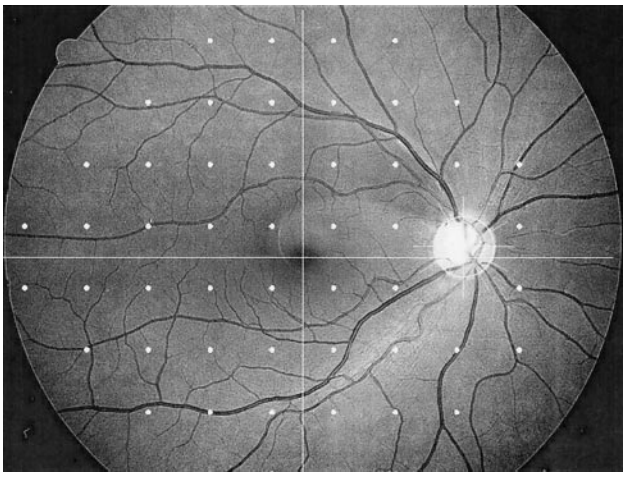

Figure 2. Example of a retinal nerve fiber layer photograph with the Humphrey 24-2 visual field test pattern and optic nerve head reference circle superimposed.

agishi et al,[13] and Anton et al[14] have reported incomplete maps relating damaged parts of the visual field to the ONH in glaucomatous eyes.

The purpose of this study was to establish the anatomical relationship between regions of the visual field and corresponding regions of the ONH by superimposing a visual field test pattern on RNFL photographs.

Methods

RNFL Photography

The archive of RNFL photographs from the Normal Tension Glaucoma Clinic at Moorfields Eye Hospital was searched for examples of photographs with discrete (focal and wedge) RNFL defects and/or prominent nerve fiber bundles, the course of which could easily be traced. Sixty-nine photographs of 69 eyes (63 patients) satisfied these criteria. If photographs of both eyes of a single patient met the criteria, both eyes were included (six patients).

Nerve fiber layer photography had been performed as part of the routine evaluation of glaucoma patients and suspects. Photographs were taken with the Canon CF60U camera (Tokyo, Japan) at the 60° field of view by use of low-sensitivity, high-resolution, black-and-white film, and a blue narrow-band interference filter. The Canon CF60U is not telecentric: the camera field of view (degrees of field per millimeter on the camera film) varies slightly with the refractive error of the eye photographed. The change in image size is approximately 1.6% per diopter of ametropia for the Canon CF60U.[15]

The photographs were digitized at a resolution of 1552 × 1164 pixels, giving a linear scaling of 26 pixels per degree in an emmetropic eye (Fig 1). The "mirror" image (about the vertical meridian) of left eyes was taken, so that all eyes in the subsequent analyses were "right eyes."

Generation of Visual Field Test Grid and Optic Disc Reference Circle

A Humphrey 24-2 test pattern (test points in a grid 6° apart) was generated digitally in Paint Shop Pro, version 5.01 (Jasc Software, Inc., Eden Prairie, MN), with the same scaling of 26 pixels per degree. The size of the test spot approximates that of a Goldmann size III target (0.43°). A circle, 152 pixels in diameter (approximately 6°—the size of an average ONH) was also generated. This was divided into 30° reference sectors.

Generation of Compound Images

The center of the test pattern grid was aligned to the fovea on the RNFL images, and the two images were digitally added. The edge of the reference circle was then aligned as closely as possible to the margins of the ONH (Elschnig's ring) and was digitally added (Fig 2). The center of the ONH was taken to be the center of the reference circle.

Estimating the Relationship between Test Points and the Optic Disc

The relationship between a test point and the ONH was determined by identifying points adjacent to the edge of an RNFL defect, or prominent bundle, and tracing the defect, or bundle, back to the ONH. The point of entry into the ONH, at the inner margin of the scleral ring of Elschnig, was determined by its relationship to the reference circle (Fig 3A, B). The temporal margin (9-o'clock position, right eye) was designated 0°, and degrees were counted in a clockwise direction. The grid point was then assigned a value in degrees according to the site of entry of the defect/bundle into the ONH. To account for the inverse relationship between retinal location and visual field location, the mirror image, about the horizontal meridian, of the test point location was recorded with the degree value of its corresponding point of entry at the ONH. The points immediately above and below the ONH were not assigned positions.

The position of the center of the ONH with respect to the fovea was recorded for each photograph.

The effect of the position of the ONH on the site of entry of defects was evaluated with stepwise multiple linear regression, with site of entry as the dependent variable and vertical and horizontal positions of the disc as independent variables, and a probability for F to enter of 0.05 and to remove of 0.10.

For comparison with previously published maps, the optic disc was divided into sectors as designated by Wirtschafter et al.[11]

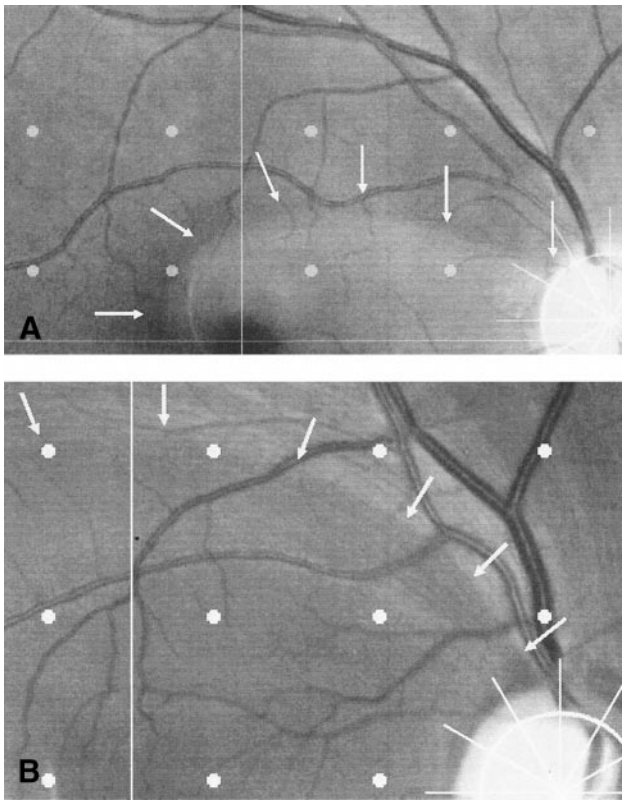

Figure 3. A and **B,** Examples of the method for estimating the corresponding optic nerve head location of visual field test points by their proximity to retinal nerve fiber layer defects.

Corresponding locations in the visual field were given the number of the disc sector for (1) Wirtschafter et al's[11] map, (2) the map corresponding to the results of this study, and (3) the partial map of Weber et al.[12]

A new map, relating visual field regions to optic disc sectors, was generated from the findings of this study.

Results

Fifty-two field test points were assigned values, representing all points in the 24-2 test grid, except those immediately above and below the ONH.

A median of 22, of a possible 69, values was assigned to each point (range, 4–58). The mean value for each point is shown in Figure 4. In general, central points and points in the arcuate bundles were assigned more values than peripheral points. The median standard deviation of assigned values was 7.2° (range, 2.6°–10.3°). No locations in particular showed greater than average variability in assigned values.

The location in the retina of the ONH was a mean 15.5° (standard deviation, 0.9°) nasal to and 1.9° (standard deviation, 1.0°) above the fovea. Figure 5 A, B illustrates the position of the ONH in relation to the fovea.

For 28 points the site of entry into the ONH was significantly correlated with the position of the ONH in relation to the fovea. Eight points were related to the horizontal position of the ONH, 10 to the vertical position, and 10 to both the horizontal and vertical position. The median r^2, for points with a significant relationship, was 0.44 (range, 0.22–0.96).

			268	262	252	245		
		264	274	281	275	260	246	
	271	285	291	296	298	283	253	229
278	287	291	298	312	329	318	.	218
83	76	68	55	34	11	13	.	167
	85	78	66	56	48	60	95	136
		88	81	77	80	93	112	
			93	95	100	108		

Figure 4. The optic nerve head location, in degrees, for each visual field test point. The temporal margin (9-o'clock position, right eye) was designated 0°, and degrees were counted in a clockwise direction.

Figure 6A shows Wirtschafter et al's divisions of the ONH into sectors. Figure 6B–D illustrates the corresponding visual field divisions derived from Wirtschafter's, this, and Weber et al's studies.

Figure 7 is a map generated from the findings of this study. It takes into account the relative positions of the optic disc and fovea: the center of the temporal optic disc segment is rotated 5° counterclockwise (downward).

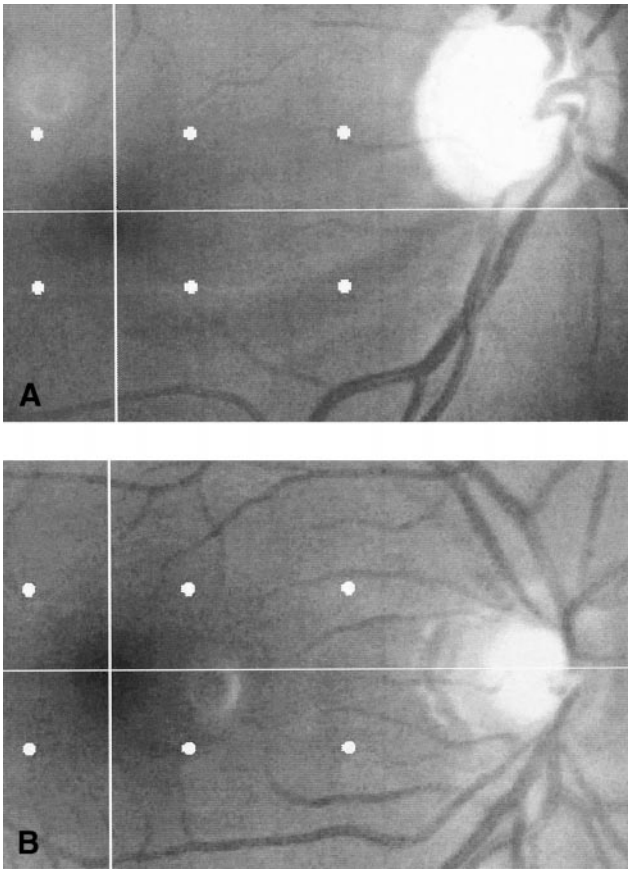

Figure 5. A and **B**, Examples of the position of the optic nerve head in relation to the fovea.

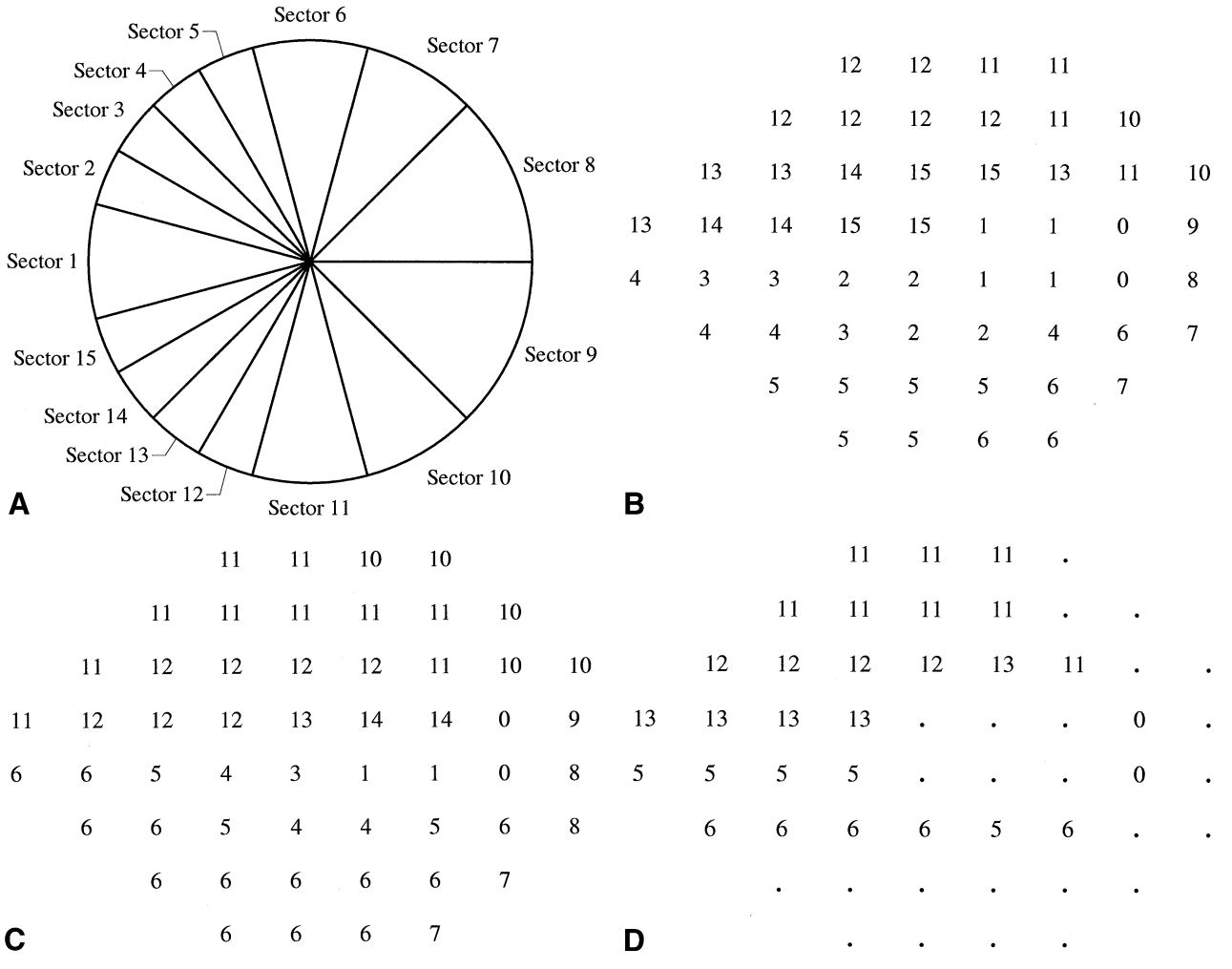

Figure 6. A, The optic nerve head divisions of Wirtschafter et al.[11] **B,** The corresponding sectors of the optic nerve head for visual field test points according to Wirtschafter et al.[11] **C,** The corresponding sectors of the optic nerve head for visual field test points according to the results of this study. **D,** The corresponding sectors of the optic nerve head for visual field test points according to the results of the Weber et al study.[12]

Discussion

The map relating visual field test points to positions at the ONH (Fig 4) is, to our knowledge, the first complete map to be derived from human RNFL images. It is compared with Wirtschafter et al's map in Figure 6. The maps differ in two significant respects. The first is that paracentral and arcuate areas of the visual field are represented by sectors nearer the poles of the ONH in the map derived from this study and by sectors nearer the temporal horizontal meridian in Wirtschafter's map. The second is that Wirtschafter et al's map is symmetric about the horizontal meridian, whereas the map in this study is slightly asymmetric, reflecting the position of the ONH above the horizontal meridian. The differences between the maps probably arise from the differences in methods, and objectives, of the studies. In Wirtschafter et al's map, the boundary lines in the visual field, which are related to sectors in the optic disc, were obtained by projecting illustrations of the primate RNFL onto an appropriately scaled visual field. The border of the "optic disc" was defined as the "physiologic blind spot," covering 13° × 9°.[16] The map was not constructed for the purpose of relating visual field sectors to ONH sectors, but to justify an anatomical basis for the subdivision of the visual field. The authors stated that the ONH sectors should be regarded as arbitrary, and not exactly related to the actual point where specific nerve fibers cross the margin of the optic disc. Despite this restriction, the map has been used as the basis for studies relating visual field test results to sectors of the optic disc.[17,18]

The map derived from this study is also compared with the partial map of Weber et al in Figure 6. The two maps show good agreement. The upper visual field test points are represented by ONH sectors slightly nearer the temporal horizontal aspect in the map derived from this study. The two maps demonstrate a similar asymmetry about the horizontal meridian. This asymmetry has also been demonstrated in visual field maps identifying functional clusters.[19]

In relating visual function in sectors of the visual field to structure in sectors of the ONH, some decision has to be

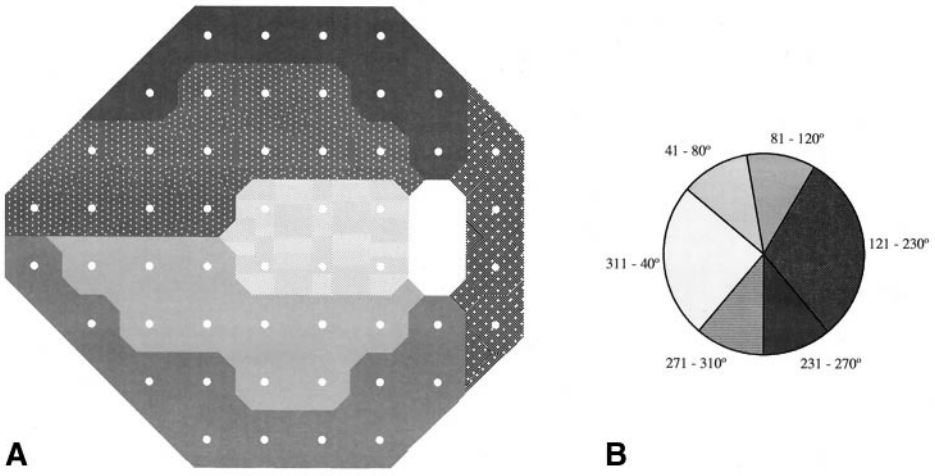

Figure 7. A division of the visual field **(A)** and optic nerve head **(B)** into sectors according to the results of this study.

made about the size of sectors. The mean variability in assigned ONH positions to visual field test points can be a guide to appropriate sector size. The mean standard deviation of assigned values was 7.2°. This means that 95% of the time a visual field test point will be associated with a position at the ONH within approximately 14° either side of a mean. In other words, the range of possible positions at the ONH covers almost 30° for each visual field test point. When clusters of field test points are considered (sectors of the visual field), ONH sector size should probably be greater than 30° to take account of this variability. The map illustrated in this article (Figure 7) consists of four 40° sectors, one 90° sector, and one 110° sector. The different sector sizes represent a compromise between minimal practical sector size and the number of visual field test points for each ONH sector.

A significant feature of the visual field test is the variability across the field in the density of test points in relation to ONH sectors. The poles of the ONH are much more densely sampled (arcuate areas of the field) than the temporal and nasal parts of the ONH (central and temporal areas of the field). This is likely to have a marked effect on the ease with which glaucomatous damage at the ONH is identified by the visual field. Criteria for glaucomatous visual field loss typically require a cluster of points with abnormal sensitivity.[20–22] If neuroretinal rim loss is focal, or uneven, the chances of obtaining a cluster of abnormal points will be greatest where the sampling is densest, that is, at the poles of the disc. It is, therefore, hardly surprising that, in early glaucoma, thinning at the poles is frequently the earliest identified sign.[23,24] Focal loss elsewhere is less likely to result in a cluster of depressed field points, and the eyes remain categorized as "ocular hypertensive" or "glaucoma suspect."

Anatomy of the RNFL

In this study, the course of RNFL defects is used to identify the region of origin of nerve fibers. An assumption is that the ganglion cell axons travel in bundles toward the ONH without any tendency to move to adjacent bundles or disperse, thereby preserving a retinotopic organization.

The organization of the ganglion cell axons in the RNFL and ONH is controversial.[25] There are two aspects that need consideration:

1. The organization of nerve fibers within the RNFL and ONH with respect to the circumferential origin of the axon;
2. The organization of nerve fibers within the RNFL and ONH with respect to the eccentricity of the origin of the axon.

Studies of the nerve fiber layer organization have been made in different species of the macaque monkey by injection of horseradish peroxidase or radioactive amino acid into the optic nerve head or retina or by making photocoagulation burns to the retina.[26–29] These have determined that a level of organization exists within the RNFL with respect to the eccentricity of the origin of the axons, although the studies do not agree on the detail. Some studies have concluded that the longer axons, from more peripheral ganglion cells, tend to lie deeper (scleral) to shorter axons,[28,29] with some intermixing.[28] Others have concluded that the axons from peripheral ganglion cells are scattered throughout the thickness of the RNFL[26] or lie in the superficial (vitreal) part of the RNFL.[27] The latter study found a degree of organization within the RNFL, with respect to eccentricity of origin, and extensive intermingling of fibers as they crossed the ONH margin. The contrasting findings in some of these studies may relate in part to species variation in RNFL organization. Stratification in the rhesus monkey has been found to be less prominent than in the owl monkey,[28] and differences between the owl monkey and macaques have been noted,[27,30] as well as differences between different species of macaque.[27,31]

These experimental studies agree that there is a clear organization with respect to the circumferential origin of axons.[27,28] Injections of horseradish peroxidase at the ONH margin result in labeling of ganglion cells in a wedge-shaped sector of retina extending into the periphery, with a

few labeled ganglion cells scattered outside this wedge-shaped sector in a larger area, estimated at less than a 2% of the total number labeled.[27] The axons of these scattered cells may correspond to the accessory fascicles described by Vrabec.[32] Axons with an aberrant intraretinal course have been identified as belonging to giant parasol-like ganglion cells.[33]

The course of ganglion cell axons has been traced in the human retina.[34,35] Some lateral movement of fibers within a fascicle was observed, but axons generally remain parallel as they approach the disc. This circumferential organization is maintained in the superficial ONH, with adjacent axons remaining in the same sector of the ONH. However, the fibers do not seem to be organized through the depth of the RNFL. Axons from most points in the retina were scattered throughout the thickness of the RNFL. Exceptions were fibers from the temporal raphé and arcuate bundles, which tended to remain deep (scleral), and a minority of fibers from the arcuate areas, which remain deep and take a more direct course to the ONH than the bulk of the fibers. A few fibers in the region of the temporal raphé may cross to the opposite hemisphere and enter the opposite side of the ONH. As the fibers enter the ONH, more superficial fibers pass to more central parts of the disc, and deeper fibers (such as those from the temporal raphé and arcuate areas) pass to more peripheral parts of the disc.

Sources of Variability

A major source of between-eye variability in the correspondence of visual field test points to ONH sectors is the position of the ONH in relation to the fovea. In more than half the test points, ONH position accounted for nearly half the interindividual variability. It is possible that some of the apparent vertical variation in the position of the ONH arises from torsion of the eye during photography, as a result of incorrect positioning of the head. This effect is likely to be small and is not likely to be greater than similar incorrect positioning of the head during perimetry. Any variability that this introduces will thus reflect the clinical situation.

Retinal magnification varies between eyes. Variation in the retinal magnification that results from interindividual variation in the size of the eye (the number of millimeters on the retina per degree of visual angle)[36] will result in differences in the absolute position (in millimeters) of the visual field test points on the retina. A change in axial length of $\pm$ 1 mm results in a change in magnification of about $\pm$5%.[36] This means that in larger eyes the visual field test points are spaced farther apart. This effect is likely to result in variation in the part of the ONH that corresponds to a given visual field test point. Application of a generalized map to eyes that may be substantially longer or shorter than average should, therefore, be done with caution.

A small source of error arises from the fact that the Canon camera is not telecentric. Refractive error data were not available for the photographs in the archive, and corrections for ametropia could, therefore, not be made. The change in image size is approximately 1.6% per diopter of ametropia for the Canon CF60U.[15] For a typical population of glaucoma patients the standard deviation of refractive error is about 2 diopters.[36] The standard deviation of change in image size is, therefore, about $\pm$3.2%. It is estimated that up to 1.2° (of the mean 7.2°) of the variability in the assignation of a disc position to field test points may be accounted for by the method (as opposed to interindividual anatomic variation), with no systematic error (bias).

In addition to variation resulting from the size of an eye, other morphological variables, such as the shape, rotation, and tilt of the ONH, are likely to lead to variation in the relationship between visual field test points and ONH sectors. It was not possible to quantify these variables in this study.

In summary, this study has produced a clinically useful map that relates visual field test points to regions of the ONH. The map will aid clinical evaluation of glaucoma patients and suspects, as well as form the basis for investigations of the relationship between retinal light sensitivity and ONH structure.

References

1. Okubo K, Mizokami K. Fundus perimetry and Octopus perimetry for the evaluation of nerve fiber layer defects. In: Heijl A, Greve EL, eds. Proceedings of the 6th International Visual Field Symposium, 1984. Dordrecht, The Netherlands: Dr. W. Junk, 1985;457–66 (Doc Ophthalmol Proc Ser; 42).
2. Westcott MC, McNaught AI, Crabb DP, et al. High spatial resolution automated perimetry in glaucoma. Br J Ophthalmol 1997;81:452–9.
3. Orzalesi N, Miglior S, Lonati C, Rosetti L. Microperimetry of localized retinal nerve fiber layer defects. Vision Res 1998; 38:763–71.
4. Betz P, Camps F, Collignon-Brach J, et al. Biometric study of the disc cup in open-angle glaucoma. Graefes Arch Clin Exp Ophthalmol 1982;218:70–4.
5. Jonas JB, Gusek GC, Naumann GOH. Optic disc, cup and neuroretinal rim size, configuration and correlations in normal eyes [published errata appear in Invest Ophthalmol Vis Sci 1991;32:1893 and 1992;32:474–5]. Invest Ophthalmol Vis Sci 1988;29:1151–8.
6. Garway-Heath DF, Hitchings RA. Quantitative evaluation of the optic nerve head in early glaucoma. Br J Ophthalmol 1998;82:352–61.
7. Mikelberg FS, Parfitt CM, Swindale NV, et al. Ability of the Heidelberg retina tomograph to detect early glaucomatous visual field loss. J Glaucoma 1995;4:242–7.
8. Wollstein G, Garway-Heath DF, Hitchings RA. Identification of early glaucoma cases with the scanning laser ophthalmoscope. Ophthalmology 1998;105:1557–63.
9. Varma R, Quigley HA, Pease ME. Changes in optic disk characteristics and number of nerve fibers in experimental glaucoma. Am J Ophthalmol 1992;114:554–9.
10. Yücel YH, Gupta N, Kalichman MW, et al. Relationship of optic disc topography to optic nerve fiber number in glaucoma. Arch Ophthalmol 1998;116:493–7.
11. Wirtschafter JD, Becker WL, Howe JB, Younge BR. Glaucoma visual field analysis by computed profile of nerve fiber function in optic disc sectors. Ophthalmology 1982;89:255–67.
12. Weber J, Dannheim F, Dannheim D. The topographical relationship between optic disc and visual field in glaucoma. Acta Ophthalmol (Copenh) 1990;68:568–74.

13. Yamagishi N, Anton A, Sample PA, et al. Mapping structural damage of the optic disk to visual field defect in glaucoma. Am J Ophthalmol 1997;123:667–76.
14. Anton A, Yamagishi N, Zangwill L, et al. Mapping structural to functional damage in glaucoma with standard automated perimetry and confocal scanning laser ophthalmoscopy. Am J Ophthalmol 1998;125:436–46.
15. Rudnicka AR, Burk RO, Edgar DF, Fitzke FW. Magnification characteristics of fundus imaging systems. Ophthalmology 1998;105:2186–92.
16. Hills JF, Wirtschafter JD, Maeder P. Boundary curves for dividing visual fields into sectors corresponding to a retinotopic projection onto the disc. In: Greve EL, Heijl A, eds. Proceedings of the Fifth International Visual Field Symposium, 1982. The Hague: Dr. W. Junk, 1983;459–64 (Doc Ophthalmol Proc Ser; 35).
17. Kono Y, Chi QM, Tomita G, et al. High-pass resolution perimetry and a Humphrey Field Analyzer as indicators of glaucomatous optic disc abnormalities. A comparative study. Ophthalmology 1997;104:1496–502.
18. Reyes RD, Tomita G, Kitazawa Y. Retinal nerve fiber layer thickness within the area of apparently normal visual field in normal-tension glaucoma with hemifield defect. J Glaucoma 1998;7:329–35.
19. Mandava S, Zulauf M, Zeyen T, Caprioli J. An evaluation of clusters in the glaucomatous visual field. Am J Ophthalmol 1993;116:684–91.
20. Åsman P, Heijl A. Glaucoma Hemifield Test. Automated visual field evaluation. Arch Ophthalmol 1992;110:812–9.
21. Åsman P, Heijl A, Olsson J, Rootzen H. Spatial analyses of glaucomatous visual fields; a comparison with traditional visual field indices. Acta Ophthalmol (Copenh) 1992;70:679–86.
22. Advanced Glaucoma Intervention Study. 2. Visual field test scoring and reliability. Ophthalmology 1994;101:1445–55.
23. Pederson JE, Anderson DR. The mode of progressive disc cupping in ocular hypertension and glaucoma. Arch Ophthalmol 1980;98:490–5.
24. Jonas JB, Fernández MC, Stürmer J. Pattern of glaucomatous neuroretinal rim loss. Ophthalmology 1993;100:63–8.
25. Caprioli J. Correlation of visual function with optic nerve and nerve fiber layer structure in glaucoma. Surv Ophthalmol 1989;33(Suppl):319–30.
26. Ogden TE. The nerve-fiber layer of the primate retina: an autoradiographic study. Invest Ophthalmol 1974;13:95–100.
27. Ogden TE. Nerve fiber layer of the macaque retina: retinotopic organization. Invest Ophthalmol Vis Sci 1983;24:85–98.
28. Radius RL, Anderson DR. The course of axons through the retina and optic nerve head. Arch Ophthalmol 1979;97:1154–8.
29. Minckler DS. The organization of nerve fiber bundles in the primate optic nerve head. Arch Ophthalmol 1980;98:1630–6.
30. Ogden TE. Nerve fiber layer of the owl monkey retina: retinotopic organization. Invest Ophthalmol Vis Sci 1983;24:265–9.
31. Radius RL, Anderson DR. The histology of retinal nerve fiber layer bundles and bundle defects. Arch Ophthalmol 1979;97:948–50.
32. Vrabec F. The temporal raphe of the human retina. Am J Ophthalmol 1966;62:926–38.
33. Thanos S, Rohrbach JM, Thiel HJ. Postmortem preservation of ganglion cells in the human retina. A morphometric investigation with the carbocyanine dye DiI. Retina 1991;11:318–27.
34. Fitzgibbon T, Taylor SF. Retinotopy of the human retinal nerve fibre layer and optic nerve head. J Comp Neurol 1996;375:238–51.
35. Fitzgibbon T. The human fetal retinal nerve fiber layer and optic nerve head: a DiI and DiA tracing study. Vis Neurosci 1997;14:433–47.
36. Garway-Heath DF, Rudnicka AR, Lowe T, et al. Measurement of optic disc size: equivalence of methods to correct for ocular magnification. Br J Ophthalmol 1998;82:643–9.

Telltale Signs

An older man with high lipids in plasma,
Said, "I want none of your razz-a-ma-tazz, Ma."
Said she, "I want you leaner,
Or I'll change my demeanor,
And leave, when your lids form their xanthelasma!"

William C. Conrad, MD